Inorganic Chemistry

Article

pubs.acs.org/IC

Selective Two-Step Oxidation of μ_2-S Ligands in Trigonal Prismatic Unit $\{Re_3(\mu_6\text{-}C)(\mu_2\text{-}S)_3Re_3\}$ of the Bioctahedral Cluster Anion $[Re_{12}CS_{17}(CN)_6]^{6-}$

Yuri V. Mironov,* Yakov M. Gayfulin, Svetlana G. Kozlova, Anton I. Smolentsev, Maria S. Tarasenko, Anton S. Nizovtsev, and Vladimir E. Fedorov

Nikolaev Institute of Inorganic Chemistry, Siberian Branch of the Russian Academy of Sciences, 3, Acad. Lavrentiev prospect, 630090, Novosibirsk, Russia

Supporting Information

ABSTRACT: An oxidation of cluster anion $[Re_{12}CS_{17}(CN)_6]^{6-}$ by H_2O_2 in water has been investigated. It was shown that selective two-step oxidation of bridging μ_2-S-ligands in trigonal prismatic unit $\{Re_3(\mu_6\text{-}C)(\mu_2\text{-}S)_3Re_3\}$ takes place. The first stage runs rapidly, whereas the speed of the second stage depends on intensity of ultraviolet irradiation of the reaction mixture. Each stage of the reaction is accompanied by a change in the solution's color. In the first stage of the oxidation, the cluster anion $[Re_{12}CS_{14}(SO_2)_3(CN)_6]^{6-}$ is produced, in which all bridging S-ligands are turned into bridging SO_2-ligands. The second stage of the oxidation leads to formation of the anion $[Re_{12}CS_{14}(SO_2)_2(SO_3)(CN)_6]^{6-}$, in which one of the SO_2-ligands underwent further oxidation forming the bridging SO_3-ligand. Seven compounds containing these anions were synthesized and characterized by a set of different methods, elemental analyses, IR and UV/vis spectroscopy, and quantum-chemical calculations. Structures of some compounds based on similar cluster anions, $[Cu(NH_3)_5]_3[Re_{12}CS_{14}(SO_2)_3(CN)_6]\cdot 9.5H_2O$, $[Ni(NH_3)_6]_3[Re_{12}CS_{14}(SO_2)_3(CN)_6]\cdot 4H_2O$, and $[Cu(NH_3)_5]_{2.6}[Re_{12}CS_{14}(SO_2)_3(CN)_6]_{0.6}[\{Re_{12}CS_{14}(SO_2)_2(SO_3)(CN)_5(\mu\text{-}CN)\}\{Cu(NH_3)_4\}]_{0.4}\cdot 5H_2O$, were investigated by X-ray analysis of single crystals.

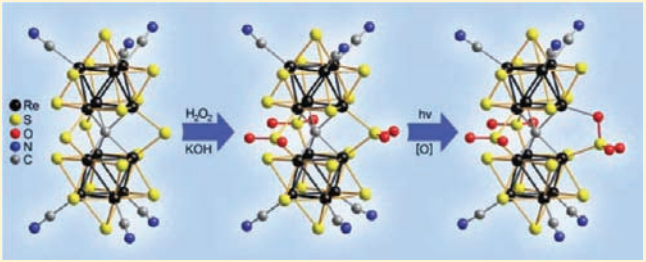

INTRODUCTION

The achievements in inorganic chemistry in the second half of the 20th century were largely related to the foundation of the basics of cluster chemistry. Complexes that contain metal clusters coordinated by chalcogenide or polychalcogenide ligands occupy a special place among numerous types of cluster compounds. Chalcogenide clusters are a typical example of so-called high-valence clusters and the most characteristic for 4d- and 5d-metals of groups 5–7.[1] Over the past 20 years, rhenium cluster complexes with four and six metal atoms have been synthesized and investigated intensively.[2] A few years ago were synthesized the first compounds with a 12-nuclear rhenium cluster core, $K_8[Re_{12}CS_{17}(CN)_6]$ and $K_6[Re_{12}CS_{17}(CN)_6]$, containing a μ_6-C-centered Re_{12} cluster unit.[3] These complexes may also be considered to be dimers composed of two Re_6 octahedrons from which the rhenium atoms of two symmetry-related triangular faces are connected through the μ_6-C interstitial carbon atom and additionally coordinated by three μ_2-S ligands. From our point of view, the central fragment of 12-nuclear rhenium clusters, $\{Re_3(\mu_6\text{-}C)(\mu_2\text{-}S)_3Re_3\}$, is the most interesting part for further investigation. For example, the removal of two electrons from the $[Re_{12}CS_{17}(CN)_6]^{8-}$ ion leads to remarkable changes in the interatomic distances in the trigonal prism, $\{Re_3(\mu_6\text{-}C)(\mu_2\text{-}S)_3Re_3\}$, which are most sensitive to the redox transformation. In the $[Re_{12}CS_{17}(CN)_6]^{8-}$ ion, the Re···Re distances in the prism are 3.168 Å, while in the oxidized complex, $[Re_{12}CS_{17}(CN)_6]^{6-}$, they are shortened to 2.902 Å. Changes in the carbon-centered fragment $\{Re_6CS_3\}$, taking place during this transformation, gave the possibility to consider these complexes as a perspective molecular switch.[4]

The most structurally closed compound containing a similar M_{12} cluster was discovered in $Ba_4Mo_{12}S_{18}$ where the l6 interstitial ligands are sulfur atoms.[5] Besides, there are some hexanuclear halogenide clusters containing W_6 prisms with interstitial C or N atoms.[6]

Here, we present our data on the oxidation of cluster anion $[Re_{12}CS_{17}(CN)_6]^{6-}$ by H_2O_2. Use of this agent leads to the oxidation of μ_2-S ligands in the prism $\{Re_3(\mu_6\text{-}C)(\mu_2\text{-}S)_3Re_3\}$ and formation of cluster anions $[Re_{12}CS_{14}(SO_2)_3(CN)_6]^{6-}$ (**1**) and $[Re_{12}CS_{14}(SO_2)_2(SO_3)(CN)_6]^{6-}$ containing new bridges, μ_2-SO_2 and μ_2-SO_3. Several compounds containing these anions, $(Ph_4P)_6[Re_{12}CS_{14}(SO_2)_3(CN)_6]$ ($(Ph_4P)_6$**1**), $K_6[Re_{12}CS_{14}(SO_2)_3(CN)_6]$ (K_6**1**), $[Cu(NH_3)_5]_3[Re_{12}CS_{14}(SO_2)_3(CN)_6]\cdot 9.5H_2O$ ($[Cu(NH_3)_5]_3$**1**),

Received: January 12, 2012
Published: March 12, 2012

   dx.doi.org/10.1021/ic300051w | *Inorg. Chem.* 2012, 51, 4359–4367

Table 1. Selected Crystal, Collection, and Refinement Data for $[Cu(NH_3)_5]_3$**1**, $[Ni(NH_3)_6]_3$**1**, and **3**

	$[Cu(NH_3)_5]_3$**1**	$[Ni(NH_3)_6]_3$**1**	**3**
empirical formula	$C_7H_{64}Cu_3N_{21}O_{15}Re_{12}S_{17}$	$C_7H_{62}N_{24}Ni_3O_{10}Re_{12}S_{17}$	$C_7H_{53.8}Cu_3N_{20.6}O_{11.4}Re_{12}S_{17}$
M	3660.83	3598.36	3579.35
space group, Z	$P\bar{1}$, 2	$R\bar{3}c$, 6	$P2_1/c$, 4
a (Å)	13.2443(7)	12.1632(6)	16.0539(5)
b (Å)	13.4391(7)		19.4392(6)
c (Å)	19.0726(9)	79.544(4)	25.4215(7)
α (deg)	84.1720(10)		
β (deg)	74.363(2)		126.296(2)
γ (deg)	77.3660(10)		
V (Å^3)	3186.7(3)	10191.4(9)	6394.1(3)
T (K)	150(2)	150(2)	150(2)
$\mu_{Mo\ K\alpha}$ (mm^{-1})	24.277	22.658	24.183
D_{calc} (g cm^{-3})	3.815	3.518	3.697
crystal size (mm)	0.12 × 0.08 × 0.03	0.20 × 0.15 × 0.05	0.12 × 0.06 × 0.06
θ scan range (deg)	1.72−27.48	2.19−26.37	1.89−27.54
measured reflns	23 904	11 145	48 415
independent reflns	13 767	2329	14 705
observed reflns [$I > 2\sigma(I)$]	10 230	2075	10 120
parameters refined	710	126	706
$R[F^2 > 2\sigma(F^2)]$, $wR(F^2)$	0.0415, 0.1123	0.0559, 0.1184	0.0458, 0.1143
$\Delta\rho_{max}$, $\Delta\rho_{min}$ (e Å^{-3})	3.990, −2.373	2.549, −2.927	4.492, −3.150

$[Ni(NH_3)_6]_3[Re_{12}CS_{14}(SO_2)_3(CN)_6]\cdot 4H_2O$ ($[Ni(NH_3)_6]_3$**1**), $(Ph_4P)_6[Re_{12}CS_{14}(SO_2)_2(SO_2/SO_3)(CN)_6]$ ($(Ph_4P)_6$**2**), $K_6[Re_{12}CS_{14}(SO_2)_2(SO_2/SO_3)(CN)_6]$ (K_6**2**), and $[Cu(NH_3)_5]_{2.6}[Re_{12}CS_{14}(SO_2)_3(CN)_6]_{0.6}[\{Re_{12}CS_{14}(SO_2)_2(SO_3)(CN)_5(\mu\text{-}CN)\}\{Cu(NH_3)_4\}]_{0.4}\cdot 5H_2O$ (**3**), were isolated and characterized. Structures of cluster compounds $[Cu(NH_3)_5]_3$**1**, $[Ni(NH_3)_6]_3$**1**, and **3** were investigated by X-ray analysis on single crystals. Composition and structure of compounds $(Ph_4P)_6$**1**, K_6**1**, $(Ph_4P)_6$**2**, and **3** were described on the basis of X-ray data for compounds $[Cu(NH_3)_5]_3$**1**, $[Ni(NH_3)_6]_3$**1**, and **3**, IR spectra, and elemental analysis.

EXPERIMENTAL SECTION

Materials and Syntheses. $K_6[Re_{12}CS_{17}(CN)_6]\cdot 20H_2O$ was prepared as previously described.[3] Commercially available reagent, 30% aqueous solution of H_2O_2, was used. Other reagents and solvents were purchased from commercial sources and used without further purification. UV/vis spectra in the wavelength range 200−1100 nm were recorded on an Ultrospec 3300 pro spectrometer. IR spectra in KBr pellets were recorded on a Bruker Scimitar FTS 2000 spectrometer in the range 4000−375 cm^{-1}. Energy dispersion spectroscopy (EDS) was performed on a scanning electron microscope (SEM) JEOL 6400. Elemental analysis was made on a Euro EA3000 analyzer.

$(Ph_4P)_6[Re_{12}CS_{14}(SO_2)_3(CN)_6]$ ($(Ph_4P)_6$1). Twenty-five milliliters of aqueous solution of H_2O_2 was added under stirring to the solution of $K_6[Re_{12}CS_{17}(CN)_6]\cdot 20H_2O$ (500 mg, 0.141 mmol) in 25 mL of water. Basic environment (pH = 9−11) was created by adding KOH to the solution of H_2O_2. After a few seconds, the color of the solution changed from dark brown to violet. Fifty milliliters of an aqueous solution, containing 400 mg (1.070 mmol) of Ph_4PCl, wsd added to the reaction mixture, resulting in the formation of purple precipitate. Mixing continued until the bleaching solution. Precipitate was separated by centrifugation and washed with water. Yield: 707 mg (nearly quantitative). Anal. Calcd for $C_{151}H_{120}N_6O_6P_6Re_{12}S_{17}$ ($(Ph_4P)_6$**1**): C, 35.70; H, 2.38; N, 1.65. Found: C, 34.40; H, 2.37; N 1.66. EDS shows the P:Re:S ratio: 6.2:12.0:16.8. FT-IR (KBr pellet, cm^{-1}): 419.1(w), 443.7(w), 524.6(s), 686.7(s), 720.9(s), 753.4(m), 995.1(s), 1019.9(s), 1106.1(s), 1163.0(m), 1184.8(m), 1436.8(s), 1481.2(w), 1583.6(w), 1652.2(w), 2116.3(s), 3056.3(w), 3424.2(m). All bands related to the PPh_4^+ cations are observed.

$K_6[Re_{12}CS_{14}(SO_2)_3(CN)_6]$ ($K_6$1). 400 mg (0.079 mmol) of $(Ph_4P)_6[Re_{12}CS_{14}(SO_2)_3(CN)_6]$ ($(Ph_4P)_6$**1**) was dissolved in 50 mL of CH_3CN. Thirty milliliters of saturated solution of KSCN in CH_3CN was added to this solution under stirring. Purple precipitate is formed on the bottom of the glass. Mixing continued until the solution was bleached. Precipitate was separated by centrifugation and washed with acetonitrile. Yield: 250 mg (quantitative). Anal. Calcd for $C_7K_6N_6O_6Re_{12}S_{17}$ (K_6**1**): C, 2.56; N, 2.56. Found: C, 2.81; N, 2.55. EDS shows the K:Re:S ratio: 5.9:12.0:16.5. FT-IR (KBr pellet, cm^{-1}): 403.4(w), 450.5(m), 5342 (m), 803.6(w), 1005.4(s), 1144.3(m), 1615.3(s), 2123.1(s), 3428.9(s), 3579.4(m).

$[Cu(NH_3)_5]_3[Re_{12}CS_{14}(SO_2)_3(CN)_6]\cdot 9.5H_2O$ ($[Cu(NH_3)_5]_3$1). A solution containing $CuCl_2\cdot 2H_2O$ (4 mg, 0.023 mmol) in 2 mL of concentrated ammonia solution was layered on a solution of K_6**1** (4 mg, 0.001 mmol) in 2 mL of water in a long tube 10 mm in diameter. After 1 month, the violet crystals of compound $[Cu(NH_3)_5]_3$**1** were formed on the tube walls. EDS shows the Cu:Re:S ratio: 3.0:12.0:16.9. FT-IR (KBr pellet, cm^{-1}): 421.8(w), 447.6(w), 527.7(m), 593.1(w), 705.3(m), 806.2(w), 1001.0(s), 1133.1(m), 1252.7(m), 1464.1(w), 1605.8(m), 1729.4(w), 2119.4(m), 2161.0(m), 2856.2(w), 2928.9(w), 2956.5(w), 3314.7(w), 3429.2(m), 3570(w).

$[Ni(NH_3)_6]_3[Re_{12}CS_{14}(SO_2)_3(CN)_6]\cdot 4H_2O$ ($[Ni(NH_3)_6]_3$1). A solution containing $NiCl_2\cdot 6H_2O$ (4 mg, 0.017 mmol) in 2 mL of concentrated ammonia solution was layered on a solution of K_6**1** (4 mg, 0.001 mmol) in 2 mL of water in a long tube 10 mm in diameter, constricted in the middle. After 1 week, the violet crystals of compound $[Ni(NH_3)_6]_3$**1** were formed on the tube walls. EDS shows the Ni:Re:S ratio: 2.9:12.2:16.9. FT-IR (KBr pellet, cm^{-1}): 426.2(w), 520.7(m), 632.7(s), 859.0(w), 923.2(w), 996.4(s), 1112.3(s), 1222.5(s), 1401.8(w), 1460.0(w), 1604.8(s), 1733.4(w), 2114.7(m), 2156.2(w), 3343.0(s).

$(Ph_4P)_6[Re_{12}CS_{14}(SO_2)_2(SO_2/SO_3)(CN)_6]$ ($(Ph_4P)_6$2). Twenty-five milliliters of aqueous solution of H_2O_2 was added under stirring to the solution of $K_6[Re_{12}CS_{17}(CN)_6]\cdot 20H_2O$ (500 mg, 0.141 mmol) in 25 mL of water. After a few seconds, the color of the solution changed from dark brown to violet. Reaction mixture was placed under sunlight. After 1 h, the color of the solution was changed from purple to green. Next, 50 mL of a solution containing 400 mg (1.070 mmol) of Ph_4PCl was added with mixing of the reaction mixture. Green precipitate appeared on the bottom of the glass. Mixing continued until the solution was bleached. Precipitate was separated by centrifugation and washed with water. Yield: 709 mg (quantitative).

dx.doi.org/10.1021/ic300051w | Inorg. Chem. 2012, 51, 4359−4367

Table 2. Characteristic Interatomic Distances (Å) for $[Cu(NH_3)_5]_3$**1**, $[Ni(NH_3)_6]_3$**1**, and **3**

	$[Cu(NH_3)_5]_3$**1**		$[Ni(NH_3)_6]_3$**1**		**3**	
bond lengths	value/range	average	value/range	average	value/range	average
Re_{in}–Re_{in}[a]	2.6396(6)–2.6563(7)	2.648(5)	2.6571(11)		2.6508(8)–2.6643(8)	2.658(5)
Re_{out}–Re_{out}	2.5955(7)–2.6076(7)	2.601(4)	2.6047(12)		2.5928(7)–2.6047(9)	2.598(4)
Re_{in}–Re_{out}	2.6040(6)–2.6253(6)	2.617(5)	2.6138(9)–2.6210(9)	2.618(4)	2.6066(7)–2.6214(8)	2.615(5)
Re···Re[b]	2.9590(6)–2.9995(6)	2.98(2)	2.9258(12)		2.9571(7)–3.0373(8)	2.99(4)
Re–μ_3-S	2.401(3)–2.438(3)	2.418(9)	2.392(4)–2.413(4)	2.404(7)	2.391(3)–2.426(4)	2.410(7)
Re–S_{SO2}	2.389(3)–2.429(3)	2.41(1)	2.390(7)		2.372(14)–2.459(15)	2.41(3)
Re–S_{SO3}					2.397(10)	
Re–μ_6-C	2.118(10)–2.157(11)	2.14(2)	2.1199(6)		2.116(14)–2.169(15)	2.14(2)
Re–C_{CN}	2.095(14)–2.136(12)	2.11(2)	2.12(2)		2.080(17)–2.112(14)	2.09(2)
Re–O					2.22(2)	
S_{SO2}–O	1.459(9)–1.497(10)	1.48(1)	1.58(2)		1.453(15)–1.51(5)	1.48(2)
S_{SO3}–O					1.46(3)–1.57(3)	1.53(6)
Ni–N			2.136(15)–2.160(16)	2.14(1)		
Cu–N	2.004(12)–2.310(12)	2.08(9)			1.976(17)–2.465(14)	2.1(1)

[a]Atoms Re_{out} and Re_{in} belong to opposite "outward" and "inward" faces of the $\{Re_6\}$ octahedron with regard to μ_6-C. [b]Distances between Re atoms in $\{Re_6C\}$ prism.

Anal. Calcd for $C_{151}H_{120}K_6N_6O_7P_6Re_{12}S_{17}$ ($(Ph_4P)_6$**2**): C, 35.59; H, 2.37; N, 1.65. Found: C, 34.70; H, 2.42; N, 1.72. EDS shows the P:Re:S ratio: 6.3:12.0:16.8. FT-IR (KBr pellet, cm^{-1}): 420.6(w), 524.9(s), 686.9(s), 721.1(s), 753.5(m), 847.7(w), 995.0(s), 1023.3(s), 1071.4(m), 1106.3(s), 1163.3(m), 1184.5(m), 1314.9(w), 1436.1(s), 1481.3(w), 1583.6(w), 1652.5(w), 2116.8(s), 3058.8(w), 3418.3(w). All bands related to the PPh_4^+ cations are observed.

$K_6[Re_{12}CS_{14}(SO_2)_2(SO_2/SO_3)(CN)_6]$ ($K_6$2). 400 mg (0.079 mmol) of $(Ph_4P)_6$**2** was dissolved in 50 mL of CH_3CN. Thirty milliliters of saturated solution of KSCN in CH_3CN was added to this solution under stirring. Green precipitate appeared on the bottom of the glass. Mixing continued until the solution was bleached. Precipitate was separated by centrifugation and washed with acetonitrile. Yield: 250 mg (quantitative). Anal. Calcd for $C_7K_6N_6O_7Re_{12}S_{17}$ (K_6**2**): C, 2.56; N, 2.56. Found: C, 2.85; N, 2.73. EDS shows the K:Re:S ratio: 6.1:12.0:16.7. FT-IR (KBr pellet, cm^{-1}): 400.2(m), 445.0(w), 534.0 (m), 671.3(m), 864.2(w), 1010.1(s), 1070.5(m), 1157.1(m), 1614.1(s), 2125.1(s), 3429.5(s), 3585.3(m).

$[Cu(NH_3)_5]_{2.6}[Re_{12}CS_{14}(SO_2)_3(CN)_6]_{0.6}[\{Re_{12}CS_{14}(SO_2)_2(SO_3)(CN)_5(\mu\text{-}CN)\}\{Cu(NH_3)_4\}]_{0.4}\cdot 5H_2O$ (3). A solution containing $CuCl_2\cdot 2H_2O$ (4 mg, 0.023 mmol) in 2 mL of concentrated ammonia solution was layered on a solution of K_6**2** (4 mg, 0.001 mmol) in 2 mL of water in a long tube 10 mm in diameter. After 6 weeks, green crystals of compound **3** formed on the tube walls. EDS shows the Cu:Re:S ratio: 3.1:12.0:17.2. FT-IR (KBr pellet, cm^{-1}): 414.6(w), 526.6(m), 580.6(w), 663.5(m), 773.4(w), 860.7(w), 1006.8(s), 1066.6(m), 1145.7(m), 1244.1(m), 1410.0(m), 1600.9(s), 2117.8(s), 2154.5(s), 2926.0(w), 3170.9(w), 3311.7(m), 3437.1(s), 3593.4(m).

Crystallography. Single-crystal X-ray diffraction data were collected with the use of graphite monochromatized Mo Kα radiation (λ = 0.71073 Å) at 150(2) K on a Bruker Nonius X8 Apex diffractometer equipped with a 4K CCD area detector. The standard φ- and φ/ω-scan techniques were employed to measure intensities. Absorption corrections were applied using the SADABS program.[7] The crystal structures were solved by direct methods and refined by full-matrix leastsquares techniques with the use of the SHELXTL software package.[8] All non-hydrogen atoms were refined anisotropically. Hydrogens of NH_3 groups were calculated by geometrical methods and refined with $U_{iso}(H) = 1.5U_{eq}(N)$; hydrogens of water molecules were not located. Crystallographic data as well as details of data collection and structure refinement for compounds $[Cu(NH_3)_5]_3$**1**, $[Ni(NH_3)_6]_3$**1**, and **3** are given in Table 1 and in the Supporting Information. Selected bond lengths are tabulated in Table 2. Complete crystallographic data have been deposited at the Inorganic Crystal Structure Database (CSD nos. 424013–424015 for compounds $[Cu(NH_3)_5]_3$**1**, $[Ni(NH_3)_6]_3$**1**, and **3**, respectively) and may be obtained free of charge via http://www.fiz-karlsruhe.de/obtaining_crystal_structure_data.html.

Computational Details. Density functional theory (DFT) calculations were carried out of the $[Re_{12}CS_{17}(CN)_6]^{6-}$, $[Re_{12}CS_{14}(SO_2)_3(CN)_6]^{6-}$, and $[Re_{12}CS_{14}(SO_2)_2(SO_3)(CN)_6]^{6-}$ cluster anions within spin-restricted formalism employing the ADF2010 program package.[9] Geometric parameters for the cluster anions considered were optimized via the Becke–Perdew general gradient approximation (GGA) exchange-correlation density functional (BP86[10]) in the gas phase. A relativistic valence triple-ζ Slater-type basis set with an augmented polarization function (TZP) without core potential was applied for all elements. The zero-order regular approximation (ZORA[11]) Hamiltonian was used in all calculations in this work to take into account the scalar relativistic effects.

To reduce computational time, the $[Re_{12}CS_{17}(CN)_6]^{6-}$ and $[Re_{12}CS_{14}(SO_2)_3(CN)_6]^{6-}$ complexes were optimized in D_{3h} symmetry, while the $[Re_{12}CS_{14}(SO_2)_2(SO_3)(CN)_6]^{6-}$ cluster was optimized in C_1 symmetry. All of the following single-point calculations were carried out with ZORA/BP86/TZP geometries. The electronic energy of model complexes was calculated using the method.[12]

The observed electronic transitions in UV/vis spectra are dipole-allowed electronic transitions according to the experimental values of extinction. To model the electronic absorption spectra, the 30 lowest-lying dipole-allowed electronic transitions were computed for each cluster within time-dependent density functional theory (TD-DFT[13]) by employing the M06-L[14] meta-GGA functional and the same basis set as that used for geometry optimization. Solvent effects on transition energies were simulated by means of the conductor-like screening model (COSMO[15]) with water as a solvent (dielectric constant equal to 78.39) using default surface parameters. From the resulting set of spectral lines, we have chosen the most intensive transitions that fall in the absorption band at 500–600 nm as the most distinctive in the experiments. The numerical integration parameter in TD-DFT calculations was set at 7.0; otherwise, default ones were used.

Topological analysis of electron density distribution within the electron localization function (ELF[16]) framework was carried out to determine the binding nature of bridging ligands μ_2-SO_2 and μ_2-SO_3 in the cluster anions under study. The ELF was calculated on a grid with a mesh size of 0.2 bohr using the ZORA/BP86/TZP wave functions.

RESULTS AND DISCUSSION

Syntheses. Compound $(Ph_4P)_6[Re_{12}CS_{14}(SO_2)_3(CN)_6]$ ($(Ph_4P)_6$**1**) was prepared by a reaction of $K_6[Re_{12}CS_{17}(CN)_6]$ with H_2O_2 in water followed by precipitation by addition of PPh_4Cl. Back reaction to the potassium salt (compound K_6**1**) has been carried out via the interaction of $(Ph_4P)_6$**1** with KSCN

dx.doi.org/10.1021/ic300051w | Inorg. Chem. 2012, 51, 4359–4367

in CH_3CN. These two stages proved to be effective for purification of compounds from H_2O_2. Finally, we obtained the single crystals of $[Cu(NH_3)_5]_3[Re_{12}CS_{14}(SO_2)_3(CN)_6]\cdot 9.5H_2O$ ($[Cu(NH_3)_5]_3$**1**) synthesized in the reaction of water solution of K_6**1** with aqueous ammonia solution of $CuCl_2$. The reaction has been performed in a thin glass tube by layering of ammonia solution of Cu^{2+} on an aqueous solution of compound K_6**1**. The single crystals of $[Ni(NH_3)_6]_3[Re_{12}CS_{14}(SO_2)_3(CN)_6]\cdot 4H_2O$ ($[Ni(NH_3)_6]_3$**1**) were obtained by a similar procedure using an ammonia solution of Ni^{2+} instead of Cu^{2+}.

Compound $K_6[Re_{12}CS_{14}(SO_2)_2(SO_2/SO_3)(CN)_6]$ (K_6**2**) was obtained on exposure of the reaction mixture (first step of preparation of $(Ph_4P)_6$**1**) to sunlight for about 1 h. The colors of solutions of K_6**1** and K_6**2** are very different. The solution of K_6**1** has a purple color, which changes to green color, characteristic of K_6**2**. Similar to the above-described procedure, purification was carried out via the precipitation of PPh_4^+ salt (compound $(Ph_4P)_6$**2**) and further reaction of $(Ph_4P)_6$**2** with KSCN in CH_3CN. Compound **3** was obtained by a reaction of K_6**2** with ammonia solution of Cu^{2+}, as described earlier.

The acetonitrile solution of $(Ph_4P)_6$**1** and water solution of K_6**1** are air-unstable under the influence of sunlight or ultraviolet and eventually become green both with and without the addition of H_2O_2. In a dark place, these solutions are stable for a long time. In inert (argon) atmosphere, the water solution of compound K_6**1** is stable under the ultraviolet lamp for a long time, so we conclude that the second stage of the oxidation process, that is, transformation of K_6**1** to K_6**2**, may proceed due to both air oxygen and H_2O_2-generated oxygen. The cluster anion $[Re_{12}CS_{14}(SO_2)_2(SO_3)(CN)_6]^{6-}$ shows greater stability; the solutions of compounds $(Ph_4P)_6$**2** and K_6**2** are not subjected to oxidation by air oxygen under the ultraviolet lamp. Yet in the presence of H_2O_2, a slow decomposition is observed through the solution color change from green to brown and then colorless. Unfortunately, no crystals were obtained from brown solutions.

The first stage of the oxidation reaction occurs only in alkaline medium (pH > 9). When trying to carry out this synthesis in neutral or acidic environment, the starting brown solution of $K_6[Re_{12}CS_{17}(CN)_6]$ becomes colorless, and characteristic changes in the profile of electronic absorption spectrum are not observed. Reaction between H_2O_2 and solution of another known Re_{12} cluster compound, $K_6[Re_{12}CS_{17}(OH)_6]$,[17] taken as a starting reagent, gave the same result. Most likely, colorless solutions contain perrhenates as final products of oxidation.

Apparently, the second stage of the reaction proceeds only partly. This suggestion is supposed by the fact that the anionic part of the compound **3** contains only 40% of the anions $[Re_{12}CS_{14}(SO_2)_2(SO_3)(CN)_6]^{6-}$, while the other 60% are the anions $[Re_{12}CS_{14}(SO_2)_3(CN)_6]^{6-}$. At present, we are unable to say the exact ratios between these anions neither in the solutions nor in the solid phases of $(Ph_4P)_6$**2** and K_6**2**.

For the sake of comparison, known compounds containing μ_2-SO_2 and μ_2-SO_3 ligands are mentioned below. The cluster complexes of Rh, Fe, Pt with μ_2-SO_2 ligands are quite common.[18] A few examples of rhenium clusters with μ_2-SO_2 ligands are also known,[19−21] while no compounds featuring μ_2-SO_3 ligands have been reported to date. All of the rhenium μ_2-SO_2 containing compounds are generally binuclear "small" clusters. Three different ways of their preparation can be found in the literature. By the first way, they can be obtained from related complexes with μ_2-S ligands through the reaction with strong oxidizing agents, for example, NO_2 and $NOPF_6$. This method has been used for the synthesis of $Re_2(\mu_2\text{-}SO_2)(\mu_2\text{-}X)X_3(CS)(dppm)_2$ (X = Cl, Br) and $[Re_2(\mu_2\text{-}SO_2)(\mu\text{-}Cl)Cl_2(CS)(dppm)_2(NCCH_3)]PF_6$.[19] Sometimes complexes containing μ_2-SO_2 ligand were discovered accidentally, as the product of the reaction with atmospheric oxygen, as it was in case of $(Et_4N)[Re_3(\mu_3\text{-}S)(\mu_2\text{-}SO_2)(\mu_2\text{-}S)_2Cl_6(PEt_3)_3]$.[20] Also, finally, a joining of SO_2 molecule to $Re_2Cl_4(\mu_2\text{-dppm})_2$ with further formation of $Re_2(\mu_2\text{-}SO_2)(\mu_2\text{-Cl})Cl_4(\mu_2\text{-dppm})_2$ is described.[21]

Although the rhenium clusters with μ_2-SO_3 ligand are not known, this ligand has been found in polynuclear complexes of many transition metals (Co, Ni, Pd, Pt, etc.). The only method of their synthesis is the association of mononuclear fragments with sulfite anion in solution. For example, the following compounds were obtained this way: $Ni[Co(en)_2(SO_3)_2]_2(H_2O)_2\cdot 4H_2O$, $[(en)Pt(SO_3)_2Pt(en)]\cdot 3H_2O$, and $[(en)Pd(SO_3)_2Pd(en)]\cdot 3H_2O$.[22] As one can see, there is a fundamental difference between this method and synthesis of the compound **3**.

Crystal Structures. Only three ($[Cu(NH_3)_5]_3$**1**, $[Ni(NH_3)_6]_3$**1**, and **3**) of all seven compounds synthesized were characterized by single-crystal X-ray diffraction analysis. Although the attempts were made to crystallize four other compounds, no crystals suitable for X-ray investigation were obtained.

$[Cu(NH_3)_5]_3[Re_{12}CS_{14}(SO_2)_3(CN)_6]\cdot 9.5H_2O$ ($[Cu(NH_3)_5]_3$1). The asymmetric unit of the triclinic structure of $[Cu(NH_3)_5]_3$**1** comprises three $[Cu(NH_3)_5]^{2+}$ cations, one cluster anion $[Re_{12}CS_{14}(SO_2)_3(CN)_6]^{6-}$, and 9.5 water molecules in 11 positions. All atoms are located in general positions (x, y, z). The structure of cluster anion $[Re_{12}CS_{14}(SO_2)_3(CN)_6]^{6-}$ is shown in Figure 1. The cluster core, $\{Re_{12}CS_{14}(SO_2)_3\}$, can be represented as two $\{Re_6\}$ octahedra linked by three μ_2-SO_2 bridging groups and one μ_6-C atom. Each $\{Re_6\}$ octahedron is embedded within a cube of seven capping μ_3-S atoms and one μ_6-C atom. Through such bonding and coordination, one can recognize μ_6-C-centered trigonal-prismatic fragment, $\{Re_3CS_3Re_3\}$, whose triangle bases belong to two adjacent $\{Re_6\}$ octahedra. Six outward Re atoms (three from each octahedron) are coordinated by terminal cyano ligands.

Most of the geometrical parameters of the anion do not differ significantly from those of the unoxidized $[Re_{12}CS_{17}(CN)_6]^{6-}$ anion in starting and related compounds[3] (Table 2). As expected, the oxidation of μ_2-S ligands affects mainly the geometry of the trigonal-prismatic fragment $\{Re_3CS_3Re_3\}$. Experimentally observed differences only take place for the Re···Re interatomic distances. The mean value of these distances is about 0.08 Å larger as compared to the value in starting salt $K_6[Re_{12}CS_{17}(CN)_6]$. The Re−($\mu_2$-S) distances show very subtle changes, which in some cases correlate with their experimental errors (i.e., 3 estimated standard deviations), but the tendency toward elongation of these bonds can be clearly identified. For the Re−(μ_6-C) bond lengths, the character of changes is analogous.

All three μ_2-SO_2 groups have the bond lengths and bond angles varying a little; they correspond well to the values reported for several metal cluster complexes containing SO_2 ligand in similar coordination mode.[18−20]

dx.doi.org/10.1021/ic300051w | Inorg. Chem. 2012, 51, 4359−4367

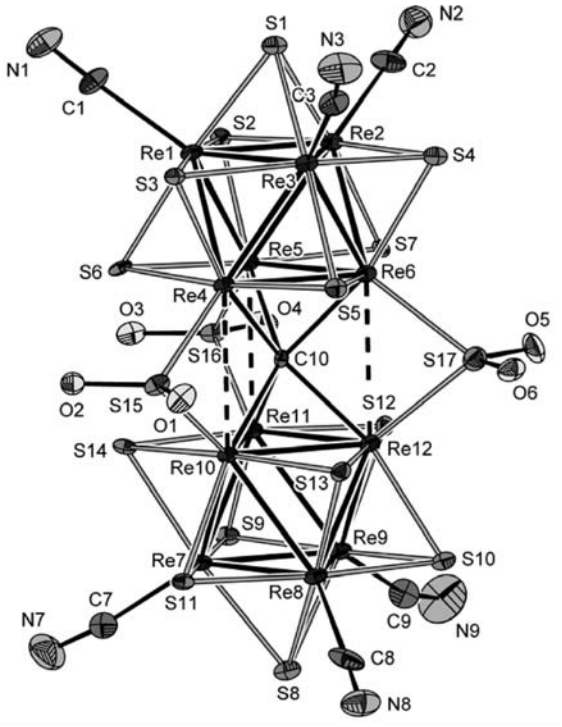

Figure 1. Structure of the cluster anion $[Re_{12}CS_{14}(SO_2)_3(CN)_6]^{6-}$ in $[Cu(NH_3)_5]_3$**1**. Thermal ellipsoids are drawn at the 40% probability level.

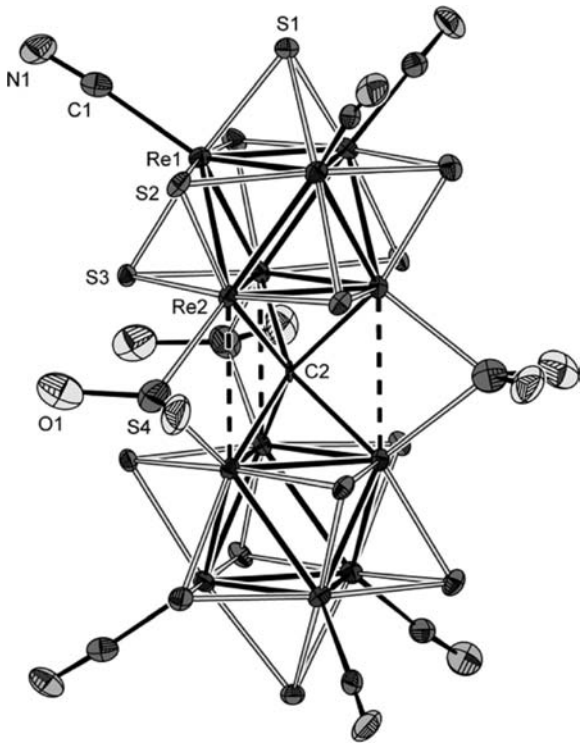

Figure 2. Structure of the cluster anion $[Re_{12}CS_{14}(SO_2)_3(CN)_6]^{6-}$ in $[Ni(NH_3)_6]_3$**1**. Only the asymmetric unit is numbered. Thermal ellipsoids are drawn at the 40% probability level.

The cationic part of the structure is represented by two types of crystallographically independent cations $[Cu(NH_3)_5]^{2+}$. The Cu atoms of the first type are five-coordinated by N atoms in a slightly distorted trigonal-bipyramidal geometry, where all Cu–N bonds are nearly equal. The second type of Cu atoms possesses a distorted tetragonal-pyramidal (4 + 1) coordination environment with basal Cu–N distances varying in the range 2.016(14)–2.080(12) Å, and apical Cu–N distances of 2.262(11) and 2.310(12) Å. Moreover, the coordination number of these Cu atoms can be increased to six (4 + 2) by a nonbonding interactions between the central atom and some of the cluster anion atoms, N atom of terminal cyano ligand or μ_3-S atom. Through the ammino H atoms, the cations form a complex network of hydrogen bonds by their association to SO_2 and CN ligands of cluster anions and lattice water molecules, obviously playing an important role in crystal lattice stabilization.

$[Ni(NH_3)_6]_3[Re_{12}CS_{14}(SO_2)_3(CN)_6]\cdot 4H_2O$ ($[Ni(NH_3)_6]_3$1). The structure of $[Ni(NH_3)_6]_3$**1** is trigonal. In the asymmetric unit, there are two independent Ni atoms lying on 3-fold (1/3, 2/3, z) and 3-fold inversion (0, 0, 0) axes; S1, S4, and C2 atoms are located on 3-fold (2/3, 1/3, z) and 2-fold (2/3, y, 1/12) axes and in a 32 special position (2/3, 1/3, 1/12), respectively (Figure 2). All other atoms occupy general positions (x, y, z). Therefore, it can be seen that the cluster anion $[Re_{12}CS_{14}(SO_2)_3(CN)_6]^{6-}$ is generated by a 2-fold axis passing through atom S4 and a 3-fold axis passing through atom S1, with both axes intersecting at the point of atom C2. The geometrical details of the anion as well as their relation to the values in the parent anion $[Re_{12}CS_{17}(CN)_6]^{6-}$ are similar to those discussed for the structure of compound $[Cu(NH_3)_5]_3$**1**.

The cations $[Ni(NH_3)_6]^{2+}$ contain the Ni atoms, which are surrounded by six N atoms originating from NH_3 coordinating ligands resulting in near octahedral geometry. These highly symmetric moieties having a large number of hydrogen atoms are effectively involved in hydrogen bonding with all acceptor groups in the structure, SO_2 and CN ligands and lattice water molecules, as it occurs in the structure of $[Cu(NH_3)_5]_3$**1**.

$[Cu(NH_3)_5]_{2.6}[Re_{12}CS_{14}(SO_2)_3(CN)_6]_{0.6}[\{Re_{12}CS_{14}(SO_2)_2(SO_3)(CN)_5(\mu\text{-}CN)\}\{Cu(NH_3)_4\}]_{0.4}\cdot 5H_2O$ (3). Compound **3** belongs to the monoclinic crystal system. The asymmetric unit contains all atoms in general positions (x, y, z). The majority of water oxygen positions are half-occupied. The key feature of this structure is the presence of two types of cluster anions sharing the same positions in the crystal lattice in a ratio of 3:2. The anion of the first (major) type has the same formula and geometry as those of the anions in the two above-described structures, that is, $[Re_{12}CS_{14}(SO_2)_3(CN)_6]^{6-}$. The anion of the second type has a more complicated structure derived from the structure of $[Re_{12}CS_{14}(SO_2)_3(CN)_6]^{6-}$. This anion contains a μ_2-SO_3 group in place of one of three μ_2-SO_2 groups and also one $\{Cu(NH_3)_4\}^{2+}$ moiety coordinated to the cluster core through the terminal CN ligand (Cu3–N8 distance is 2.44(2) Å). Thus, the formula of this anion should be $[\{Re_{12}CS_{14}(SO_2)_2(SO_3)(CN)_5(\mu\text{-}CN)\}\{Cu(NH_3)_4\}]^{4-}$ (Figure 3).

As it is seen from Figure 3, the μ_2-SO_3 group contains the atoms O7 and S17, each coordinated to rhenium atoms Re5 and Re11 at the distances of 2.22(2) and 2.397(10) Å, respectively. Through this coordination, the composition of μ_6-C-centered prismatic fragment transforms from $\{Re_6CS_3\}$ to $\{Re_6CS_3O\}$. Note that the appearance of SO_3 group in such a role is unprecedented for the rhenium cluster complexes. A detailed comparison of two types of cluster anions reveals that despite replacement of one μ_2-SO_2 group by a μ_2-SO_3 group, the geometry of the μ_6-C-centered prismatic fragment remained almost unaffected. The Re···Re, Re–(μ_2-S), and Re–(μ_6-C)

dx.doi.org/10.1021/ic300051w | Inorg. Chem. 2012, 51, 4359–4367

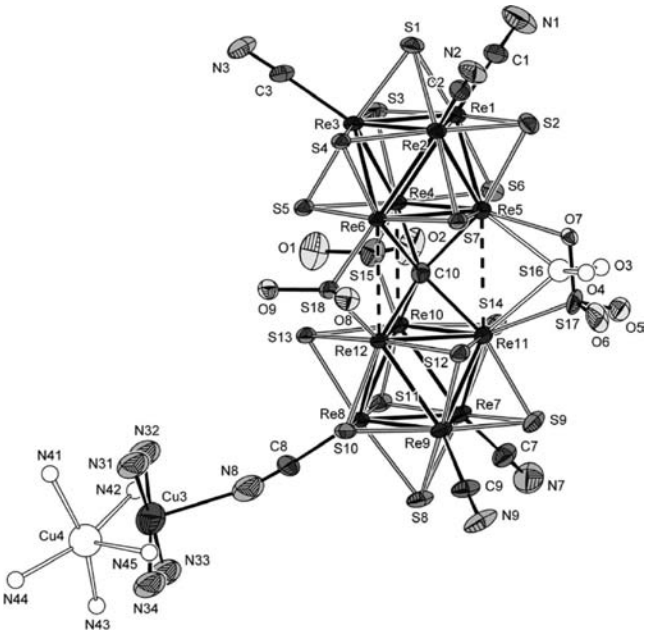

Figure 3. Structure of the cluster anion $[\{Re_{12}CS_{14}(SO_2)_2(SO_3)(CN)_5(\mu\text{-}CN)\}\{Cu(NH_3)_4\}]^{4-}$ in **3**. Thermal ellipsoids are drawn at the 30% probability level. Hydrogen atoms of the NH_3 ligands are omitted for clarity. Atoms corresponding to the copresent anion $[Re_{12}CS_{14}(SO_2)_3(CN)_6]^{6-}$ are depicted in white.

distances are in agreement with those observed in the above-described structures (Table 2).

Describing the anion $[\{Re_{12}CS_{14}(SO_2)_2(SO_3)(CN)_5(\mu\text{-}CN)\}\{Cu(NH_3)_4\}]^{4-}$, it is necessary to explain the presence of $\{Cu(NH_3)_4\}^{2+}$ fragment within it. The coexistence of this Cu3-based fragment and μ_2-SO_3 group is determined by the fact of structural inconsistency between the sulfito group and Cu3-counterpart, the Cu4-based cation $[Cu(NH_3)_5]^{2+}$, whose atom N45 (symmetry generated, not shown in Figure 3) "collides" with the O6 atom at a short distance of about 2.4 Å. Consequently, the later pentammino cation can coexist only with the "SO_3-free" anion, that is, $[Re_{12}CS_{14}(SO_2)_3(CN)_6]^{6-}$. On the other hand, the ratio of both anions is based on the results of free variable (FVAR) refinement of Cu3 and Cu4 site occupancies, which after rounding were 0.4 versus 0.6, respectively.

The discrete $[Cu(NH_3)_5]^{2+}$ cations that compensate the anionic part of the structure contain the Cu atoms in a distorted tetragonal-pyramidal (4 + 1) coordination environment with basal Cu−N distances ranging from 1.976(17) to 2.060(10) Å and apical Cu−N distances of 2.465(14), 2.282(16), and 2.32(4) Å. Similarly to the structure of $[Cu(NH_3)_5]_3$**1**, the coordination sphere of the Cu atoms can be extended by additional cyano N atoms or μ_3-S atom, distanced at about 2.5, 2.8, and 3.3 Å, respectively. All of the H atoms of the cations are involved in a complex network of hydrogen bonds stabilizing the structure.

IR Spectroscopy. In the IR spectra of all seven compounds, the absorption band characteristic for CN ligands is observed as a single line in the interval 2116—2125 cm^{-1}. Most interesting for our investigation is the area related to the vibrations of μ_2-SO_2 and μ_2-SO_3 groups, which typically lie at 900−1200 cm^{-1}. In Figure 4 are shown IR spectra of compounds K_6**1** and K_6**2**. In the spectra of compound K_6**1**, which contains only μ_2-SO_2 groups, there are two intensive lines at 1005 and 1143 cm^{-1}. In

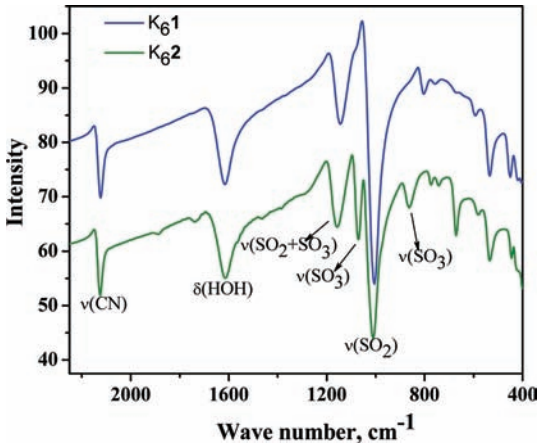

Figure 4. IR spectra of compounds K_6**1** and K_6**2**.

the spectra of compound K_6**2**, containing both μ_2-SO_2 and μ_2-SO_3 groups, lines are observed at 864, 1008, 1070, and 1157 cm^{-1}. The same situation is observed for all listed compounds. On the basis of the literature data, we can assume that bridging SO_3 ligand appears in bands at 1070 and 864 cm^{-1}, and one more band at 1143−1157 cm^{-1} is overlapped with band from μ-SO_2 ligands. The band at about 1000 cm^{-1} corresponds to the vibrations of SO_2 groups.[19−23]

UV/Vis Spectroscopy. Oxidation process is characterized by a sharp change in the profile of electronic absorption spectrum. In the spectrum of starting compound, $K_6[Re_{12}CS_{17}(CN)_6]$, in area 400—800 nm there are two broad absorption bands, roughly at 440 nm with $\varepsilon = 8.8 \times 10^3$ and 510 nm with $\varepsilon = 5.7 \times 10^3$. In the spectra of compounds K_6**1** and K_6**2**, there are bands at 529 and 592 nm with $\varepsilon = 7.5 \times 10^3$ and $\varepsilon = 5.4 \times 10^3$, respectively. As stated above, the first stage of the oxidation (obtaining of the compound K_6**1**) proceeds very rapidly. In contrast to that, the second stage (obtaining of the compound K_6**2**) proceeds much slower. It takes 1−2 min of sunlight exposure for the visible changes in water solution of K_6**1** and H_2O_2 to appear. The experiment to confirm the influence of irradiation has been carried out. The reaction mixture containing $K_6[Re_{12}CS_{17}(CN)_6]$ and H_2O_2 in water was exposed to sunlight for about 60 s. UV/vis spectra after each irradiation test were collected. Observations were stopped after three simple profiles obtained. The results received are demonstrated in Figure 5. It is clearly shown that the intensity of the absorption band with the maximum at

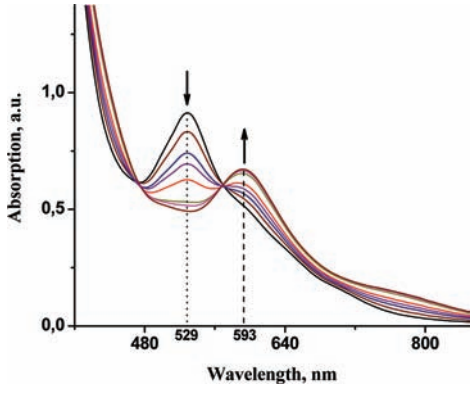

Figure 5. UV/vis spectra transformation during the oxidation of $[Re_{12}CS_{14}(SO_2)_3(CN)_6]^{6-}$ to $[Re_{12}CS_{14}(SO_2)_2(SO_3)(CN)_6]^{6-}$.

dx.doi.org/10.1021/ic300051w | Inorg. Chem. 2012, 51, 4359−4367

Table 3. Selected Interatomic Distances (Å) and Bonding Energies (ΔE, eV) for Cluster Anions $[Re_{12}CS_{17}(CN)_6]^{6-}$, $[Re_{12}CS_{14}(SO_2)_3(CN)_6]^{6-}$, and $[Re_{12}CS_{14}(SO_2)_2(SO_3)(CN)_6]^{6-}$ in the Gas Phase and in Water Solution (in Parentheses)

cluster anion	Re···Re	Re−(μ_2-S)	Re−(μ_6-C)	(μ_6-C)−S	Re−O
$[Re_{12}CS_{17}(CN)_6]^{6-}$ ΔE = −309.1 (−375.6)	2.974	2.391	2.171	3.454	
$[Re_{12}CS_{14}(SO_2)_3(CN)_6]^{6-}$ ΔE = −346.8 (−416.4)	3.075	2.509	2.179	3.527	
$[Re_{12}CS_{14}(SO_2)_2(SO_3)(CN)_6]^{6-}$ ΔE = −353.4 (−423.6)	3.236	2.518	2.194 av	3.858	2.098
	3.039	2.501		3.559	
	3.040	2.508		3.558	

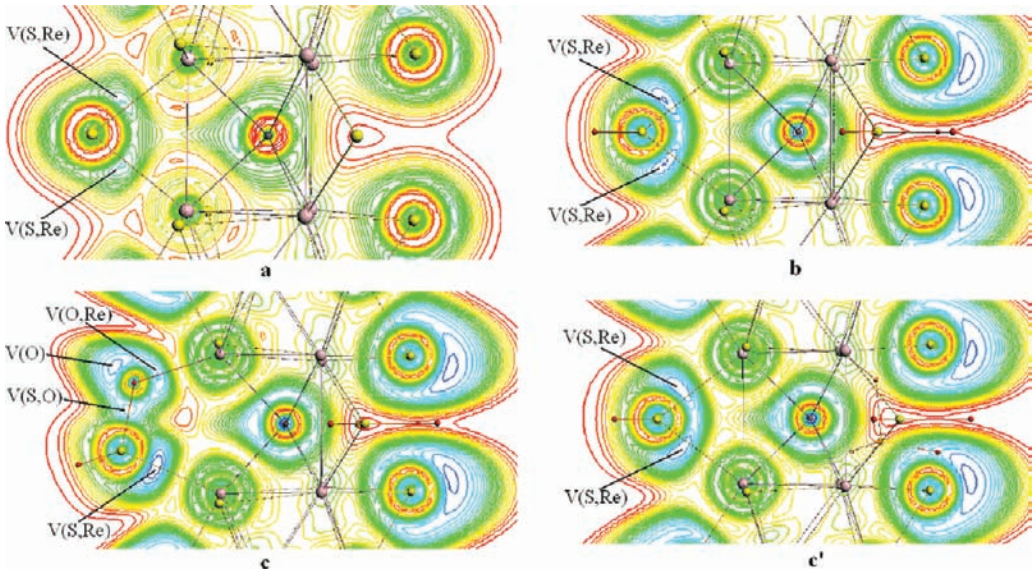

Figure 6. ELF maps for $[Re_{12}CS_{17}(CN)_6]^{6-}$ (a, cutting plane Re−(μ_2-S)−Re−(μ_6-C)), $[Re_{12}CS_{14}(SO_2)_3(CN)_6]^{6-}$ (b, cutting plane Re−S_{SO2}−Re−(μ_6-C)), and $[Re_{12}CS_{14}(SO_2)_2(SO_3)(CN)_6]^{6-}$ (c, cutting plane Re−S_{SO3}−Re−(μ_6-C); and c′, cutting plane Re−S_{SO2}−Re−(μ_6-C)) complexes. V(S,Re), V(S,O), and V(O,Re) are disynaptic basins (covalent and dative bonds) between S−Re, S−O, and O−Re; V(O) is a monosynaptic basin (lone electron pairs of O).

529 nm, typical for solution of K_6**1**, decreases with time. The intensity of the band with the maximum at 592 nm, by contrast, increases, which indicates a gradual growth of concentration of $[Re_{12}CS_{14}(SO_2)_2(SO_3)(CN)_6]^{6-}$ anions.

Density Functional Theory (DFT) Calculations. *Geometric Parameters and Bonding Energy.* Optimized geometrical parameters of the complexes $[Re_{12}CS_{17}(CN)_6]^{6-}$, $[Re_{12}CS_{14}(SO_2)_3(CN)_6]^{6-}$, and $[Re_{12}CS_{14}(SO_2)_2(SO_3)(CN)_6]^{6-}$ are presented in Table 3. Good agreement between calculated and experimental data is obtained (see experimental results). According to calculations, the electronic energy of bonding (ΔE) of complexes is characterized by negative values (Table 3).

Interatomic Interaction in {Re_6CS_3}, {$Re_6C(SO_2)_3$}, and {$Re_6C(SO_2)_2(SO_3)$} Polyhedra. The maps of ELF for $[Re_{12}CS_{17}(CN)_6]^{6-}$, $[Re_{12}CS_{14}(SO_2)_3(CN)_6]^{6-}$, and $[Re_{12}CS_{14}(SO_2)_2(SO_3)(CN)_6]^{6-}$ complexes are shown in Figure 6. As shown earlier,[24] the ion μ_6-C in the complex $[Re_{12}CS_{17}(CN)_6]^{6-}$ is characterized by sp^2-hybridization (Figure 6a). Maps of ELF function for $[Re_{12}CS_{14}(SO_2)_3(CN)_6]^{6-}$ and $[Re_{12}CS_{14}(SO_2)_2(SO_3)(CN)_6]^{6-}$ complexes demonstrate that the ion μ_6-C is also able to sp^2-hybridize (Figure 6b,c,c′). It should be noted that μ_6-C is not located in a trigonal symmetry in $[Re_{12}CS_{14}(SO_2)_2(SO_3)(CN)_6]^{6-}$ complex. However, the distances between μ_6-C and the nearest of S and Re atoms show that the symmetry environment of the μ_6-C can be regarded as a pseudo trigonal (see Tables 2 and 3). Apparently, ELF shows this. The nature of the bonding between atoms Re and S in all three complexes is dative. It is determined by the position of disynaptic basins V(S,Re) on S−Re bonds. One can see that the maximum localization basins V(S,Re), V(O,Re) located on the direct lines of S−Re and O−Re bonds of μ_2-SO_3 group, while the maximum localization basins V(S,Re) are displaced from the direct lines of S−Re bonds of μ_2-SO_2 and μ_2-S groups. The latter may indicate that the μ_2-SO_2 and μ_2-S groups form a tense (banana) bond with Re atoms, and their binding with complexes is of more relaxed character than μ_2-SO_3 groups.

Analysis of UV/Vis Spectra. The calculated most intensive electronic transitions are shown together with the experimental absorption bands (Figure 7, Table 4) .

For $[Re_{12}CS_{17}(CN)_6]^{6-}$ complex, the experimental value of the maximum of absorption band (508 nm) corresponds to the calculated electronic transition with high intensity from HOMO−1 to LUMO+5 (Figure 8). The transition can be characterized as a transfer of an electron from the valence p-orbitals of the bridging S atoms to the valence d-orbitals of the Re atoms; thus, it can be assigned to ligand-to-metal charge transfer (LMCT).

The electronic transitions under study in $[Re_{12}CS_{14}(SO_2)_3(CN)_6]^{6-}$ and $[Re_{12}CS_{14}(SO_2)_2(SO_3)(CN)_6]^{6-}$ are more complicated. In particular, for $[Re_{12}CS_{14}(SO_2)_3(CN)_6]^{6-}$ complex, the experimental absorption band at 529 nm may be due to the intense electronic

dx.doi.org/10.1021/ic300051w | Inorg. Chem. 2012, 51, 4359−4367

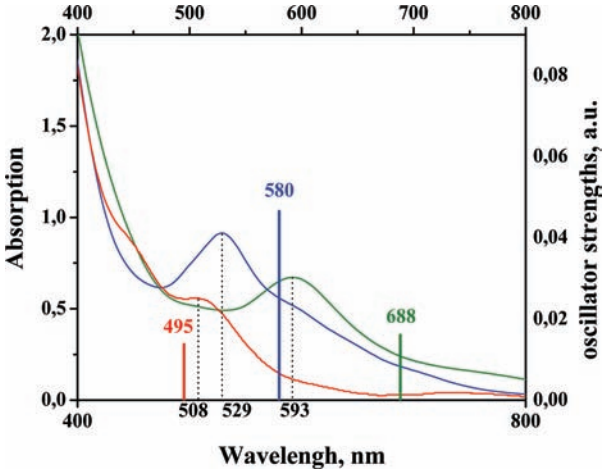

Figure 7. Colored solid vertical lines: The estimated maximum intensity allowed dipole transitions. Red color, $[Re_{12}CS_{17}(CN)_6]^{6-}$; blue color, $[Re_{12}CS_{14}(SO_2)_3(CN)_6]^{6-}$; and green color, $[Re_{12}CS_{14}(SO_2)_2(SO_3)(CN)_6]^{6-}$.

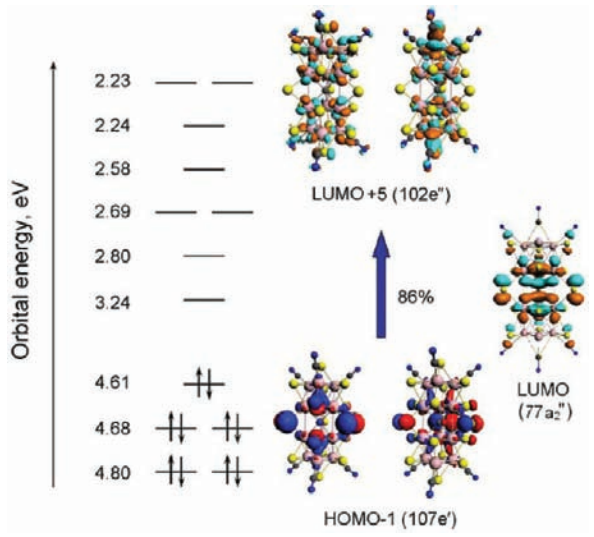

Figure 8. The schematic view of the MO levels and MOs involved in the most intensive electronic transition for $[Re_{12}CS_{17}(CN)_6]^{6-}$ complex.

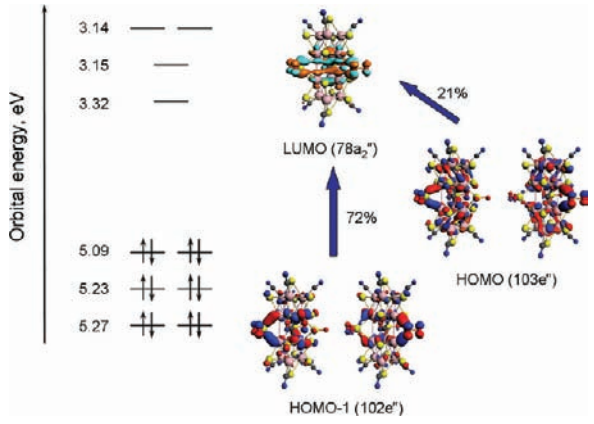

Figure 9. The schematic view of the MO levels and MOs involved in the most intensive electronic transition for $[Re_{12}CS_{14}(SO_2)_3(CN)_6]^{6-}$ complex.

transition from the HOMO−1 (72%) and HOMO (21%) levels to the LUMO level (Figure 9). $[Re_{12}CS_{14}(SO_2)_2(SO_3)(CN)_6]^{6-}$ anion, in turn, has the experimental absorption band at 593 nm that may be due to the intense electronic transition from HOMO−2 (59%) and HOMO (22%) levels to LUMO (Figure 10). In both cases, relevant MOs are mainly comprised of p- and d-orbitals of S (from bridging SO_2-ligands) and Re atoms, respectively. So, inspecting components of corresponding MOs, we can assign both transitions to the metal-to-metal charge transfer (MMCT) with smaller contribution of metal-to-ligand charge transfer (MLCT).

Note that complexes $[Re_{12}CS_{14}(SO_2)_3(CN)_6]^{6-}$ and $[Re_{12}CS_{14}(SO_2)_2(SO_3)(CN)_6]^{6-}$ are characterized by electron transitions to LUMO ($78a_2''$) and LUMO (660a) in visible region. In $[Re_{12}CS_{17}(CN)_6]^{6-}$, the LUMO ($77a_2''$) level has an electronic structure close to LUMO ($78a_2''$) and LUMO (660a) (Figures 8, 9, and 10). When the complex $[Re_{12}CS_{17}(CN)_6]^{6-}$ is reduced to complex $[Re_{12}CS_{17}(CN)_6]^{8-}$, the LUMO ($77a_2''$) being filled by two electrons. The process is associated with an abrupt increase of $Re_{in}-Re_{in}$ distances.[3] Therefore, one-electron excitation of complexes $[Re_{12}CS_{14}(SO_2)_3(CN)_6]^{6-}$ and $[Re_{12}CS_{14}(SO_2)_2(SO_3)(CN)_6]^{6-}$ in our experiments is expected to be associated with an increase of $Re_{in}-Re_{in}$ distances as well.

In conclusion, an original road of selective oxidation of bridging sulfide ligands in bioctahedral cluster complex $[Re_{12}CS_{17}(CN)_6]^{6-}$ has been discovered. Two new anions containing SO_2 and SO_3 ligands, $[Re_{12}CS_{14}(SO_2)_3(CN)_6]^{6-}$ and $[Re_{12}CS_{14}(SO_2)_2(SO_3)(CN)_6]^{6-}$, were isolated and characterized. Seven novel compounds based on these bioctahedral rhenium cluster anions were synthesized and studied by a set of different methods, elemental analyses, X-ray diffraction, IR and UV/vis spectroscopy, and quantum-chemical calculations. The results obtained demonstrate a high stability of Re_{12} clusters in redox reactions as a whole and, in particular, show high stability of terminal CN ligands. Normally, terminal ligands are more reactive as compared to inner ligands located in the cluster core. On the other hand, such an oxidant as H_2O_2 in basic solutions is often used for the decomposition of cluster complexes for further chemical analyses. These experiments open a new way for chemical modification of cluster complexes with similar type of coordination of sulfide ligands.

Table 4. Excitation Energies, Oscillator Strengths (f), and Main Transition Configurations for the Most Intensive Transitions between 500 and 700 nm for the Cluster Anions Considered Computed at the ZORA/COSMO/TD-M06-L/TZP//ZORA/BP86/TZP Level

cluster anion	excitation	f	transition	expt.
$[Re_{12}CS_{17}(CN)_6]^{6-}$	2.50 eV (495 nm)	0.014	HOMO−1→LUMO+5 (86%)	2.44 eV (508 nm)
$[Re_{12}CS_{14}(SO_2)_3(CN)_6]^{6-}$	2.14 eV (580 nm)	0.047	HOMO−1→LUMO (72%), HOMO→LUMO (21%)	2.34 eV (529 nm)
$[Re_{12}CS_{14}(SO_2)_2(SO_3)(CN)_6]^{6-}$	1.80 eV (688 nm)	0.016	HOMO−2→LUMO (59%), HOMO→LUMO (22%)	2.09 eV (593 nm)

dx.doi.org/10.1021/ic300051w | Inorg. Chem. 2012, 51, 4359−4367

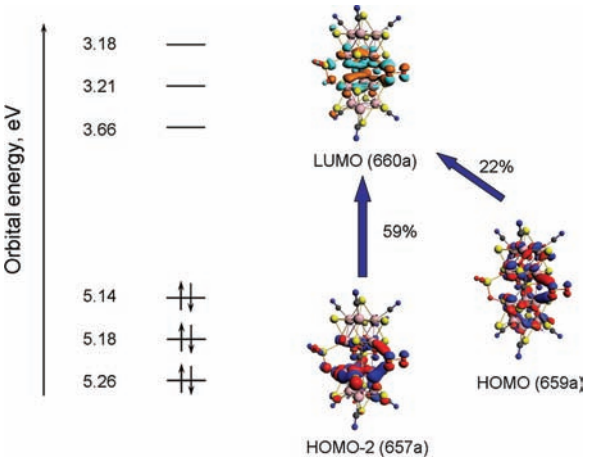

Figure 10. The schematic view of the MO levels and MOs involved in the most intensive electronic transition for $[Re_{12}CS_{14}(SO_2)_2(SO_3)(CN)_6]^{6-}$ complex.

■ ASSOCIATED CONTENT

Supporting Information

Crystallographic information in CIF format. This material is available free of charge via the Internet at http://pubs.acs.org.

■ AUTHOR INFORMATION

Corresponding Author

*E-mail: yuri@niic.nsc.ru.

Notes

The authors declare no competing financial interest.

■ ACKNOWLEDGMENTS

This research was supported by the Russian Foundation for Basic Research (grants 10-03-01040 and 11-03-00637) and by the State Contract No. 02.740.11.0628. A.S.N. acknowledges support from the program of the Russian Government "Research and educational personnel of innovative Russia" (Contract No. 14.740.12.1379).

■ REFERENCES

(1) (a) Gray, T. G. *Coord. Chem. Rev.* **2003**, *243*, 213−235. (b) Fedorov, V. E.; Mironov, Y. V.; Naumov, N. G.; Sokolov, M. N.; Fedin, V. P. *Russ. Chem. Rev.* **2007**, *76*, 529−552. (c) Perrin, A.; Perrin, C. *Eur. J. Inorg. Chem.* **2011**, 3848−3856.

(2) (a) Mironov, Y. V.; Virovets, A. V.; Fedorov, V. E.; Podberezskaya, N. V.; Shishkin, O. V.; Struchkov, Y. T. *Polyhedron* **1995**, *14*, 3171−3173. (b) Lougui, A.; Mironov, Y. V.; Perrin, A.; Fedorov, V. E. *Croat. Chem. Acta* **1995**, *68*, 885−890. (c) Beauvais, L. G.; Shores, M. P.; Long, J. R. *Chem. Mater.* **1998**, *10*, 3783−3786. (d) Gabriel, J.-C. P.; Boubekeur, K.; Uriel, S.; Batail, P. *Chem. Rev.* **2001**, *101*, 2037−2066. (e) Selby, H. D.; Roland, B. K.; Zheng, Z. *Acc. Chem. Res.* **2003**, *36*, 933−944. (f) Efremova, O. A.; Mironov, Y. V.; Fedorov, V. E. *Eur. J. Inorg. Chem.* **2006**, 2533−2549.

(3) Mironov, Y. V.; Naumov, N. G.; Kozlova, S. G.; Kim, S.-J.; Fedorov, V. E. *Angew. Chem., Int. Ed.* **2005**, *44*, 6867−6871.

(4) Gabuda, S. P.; Kozlova, S. G.; Mironov, Y. V.; Fedorov, V. E. *Nanoscale Res. Lett.* **2009**, *4*, 1110−1114.

(5) Salloum, D.; Gautier, R.; Potel, M.; Gougeon, P. *Angew. Chem., Int. Ed.* **2005**, *44*, 1363−1365.

(6) (a) Welch, E. J.; Yu, C. L.; Crawford, N. R. M.; Long, J. R. *Angew. Chem., Int. Ed.* **2005**, *44*, 2549−2553. (b) Weisser, M.; Tragl, S.; Meyer, H.-J. *J. Cluster Sci.* **2009**, *20*, 249−258.

(7) *APEX2 (Version 1.08), SAINT (Version 7.03), SADABS (Version 2.11)*; Bruker AXS Inc.: Madison, WI, 2004.

(8) Sheldrick, G. M. *Acta Crystallogr.* **2008**, *A64*, 112−122.

(9) (a) te Velde, G.; Bickelhaupt, F. M.; van Gisbergen, S. J. A.; Fonseca Guerra, C.; Baerends, E. J.; Snijders, J. G.; Ziegler, T. *J. Comput. Chem.* **2001**, *22*, 931−967. (b) Fonseca Guerra, C.; Snijders, J. G.; te Velde, G.; Baerends, E. J. *Theor. Chem. Acc.* **1998**, *99*, 391−403. (c) *ADF2010.02 SCM, Theoretical Chemistry*; Vrije Universiteit: Amsterdam, The Netherlands; http://www.scm.com.

(10) (a) Becke, A. D. *Phys. Rev. A* **1988**, *38*, 3098−3100. (b) Perdew, J. P. *Phys. Rev. B* **1986**, *33*, 8822−8824.

(11) (a) van Lenthe, E.; Ehlers, A. E.; Baerends, E. J. *J. Chem. Phys.* **1999**, *110*, 8943−8954. (b) van Lenthe, E.; Baerends, E. J.; Snijders, J. G. *J. Chem. Phys.* **1993**, *99*, 4597−4611. (c) van Lenthe, E.; Baerends, E. J.; Snijders, J. G. *J. Chem. Phys.* **1994**, *101*, 9783−9800. (d) van Lenthe, E.; Snijders, J. G.; Baerends, E. J. *J. Chem. Phys.* **1996**, *105*, 6505−6517. (e) van Lenthe, E.; van Leeuwen, R.; Baerends, E. J.; Snijders, J. G. *Int. J. Quantum Chem.* **1996**, *57*, 281−293.

(12) (a) Bickelhaupt, F. M.; Baerends, E. J. In *Reviews in Computational Chemistry*; Lipkowitz, K. B., Boyd, D. B., Eds.; Wiley: New York, 2000; Vol. *15*, pp 1−86. (b) Ziegler, T.; Rauk, A. *Inorg. Chem.* **1979**, *18*, 1558−1565.

(13) Casida, M. E. In *Recent Advances in Density Functional Methods*; Chong, D. P., Eds.; Word Scientific: Singapore, 1995; Vol. *1*, pp 155−192.

(14) Zhao, Y.; Truhlar, D. G. *J. Chem. Phys.* **2006**, 125.

(15) (a) Pye, C. C.; Ziegler, T. *Theor. Chem. Acc.* **1999**, *101*, 396−408. (b) Klamt, A.; Schüürmann, G. *J. Chem. Soc., Perkin Trans.* **1993**, *2*, 799−805. (c) Klamt, A. *J. Phys. Chem.* **1995**, *99*, 2224−2235. (d) Klamt, A.; Jones, V. *J. Chem. Phys.* **1996**, *105*, 9972−9981.

(16) (a) Becke, A. D.; Edgecombe, K. E. *J. Chem. Phys.* **1990**, *92*, 5379−5403. (b) Silvi, B.; Savin, A. *Nature* **1994**, *371*, 683−686.

(17) Mironov, Y. V.; Kozlova, S. G.; Kim, S.-J.; Sheldrick, W. S.; Fedorov, V. E. *Polyhedron* **2010**, *29*, 3283−3286.

(18) (a) Nakajima, T.; Konomoto, H.; Ogawa, H.; Wakatsuki, Y. *J. Organomet. Chem.* **2007**, *692*, 4886−4894. (b) Churchill, M. R.; Kalra, K. L. *Inorg. Chem.* **1973**, *12*, 1650−1656. (c) Briant, C. E.; Theobald, B. R. C.; Mingos, D. M. P. *J. Chem. Soc., Chem. Commun.* **1981**, 963−965. (d) Bogdan, P. L.; Sabat, M.; Sunshine, S. A.; Woodcock, C.; Shriver, D. F. *Inorg. Chem.* **1988**, *27*, 1904−1910. (e) Burrows, A. D.; Mingos, D. M. P.; Powell, H. R. *J. Chem. Soc., Dalton Trans.* **1992**, 261−268. (f) Burrows, A. D.; Choi, N.; McPartlin, M.; Mingos, D. M. P.; Tarlton, S. V.; Vilar, R. *J. Organomet. Chem.* **1999**, *573*, 313−322. (g) Arifhodzic-Radojevic, S.; Burrows, A. D.; Choi, N.; McPartlin, M.; Mingos, D. M. P.; Tarlton, S. V.; Vilar, R. *J. Chem. Soc., Dalton Trans.* **1999**, 3981−3988.

(19) Schrier, P. W.; Fanwick, P. E.; Walton, R. *Inorg. Chem.* **1992**, *31*, 3929−3933.

(20) Sokolov, M.; Imoto, H.; Saito, T. *Chem. Lett.* **1998**, *27*, 949−950.

(21) Ganesan, M.; Fanwick, P. E.; Walton, R. A. *Inorg. Chim. Acta* **2003**, *343*, 391−394.

(22) (a) Hong, K.-P.; Park, H. S.; Kwon, Y.-U. *Bull. Korean Chem. Soc.* **1999**, *20*, 163−168. (b) Krieglstein, R.; Breitinger, D. K.; Liehr, G. *Eur. J. Inorg. Chem.* **2001**, 3067−3072.

(23) Nakamoto, K. *Infrared and Raman Spectra of Inorganic and Coordination Compounds*, 5th ed.; John Wiley and Sons: New York, 1997.

(24) Kozlova, S. G.; Gabuda, S. P.; Slepkov, V. A.; Mironov, Y. V.; Fedorov, V. E. *Polyhedron* **2008**, *27*, 3167.